

# Machine Learning in Remote Sensing

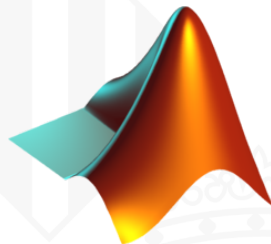
## –Practice material–

**Gustau Camps-Valls**

Image Processing Laboratory (IPL) – Universitat de València  
[gustau.camps@uv.es](mailto:gustau.camps@uv.es) — <http://isp.uv.es>



- ① Supervised classification of hyperspectral images
- ② Feature extraction from hyperspectral images
- ③ Spectral unmixing and abundance estimation
- ④ Hyperspectral and LiDAR data fusion
- ⑤ Biophysical parameter retrieval with kernel regression



**Practice 1:** Supervised classification of hyperspectral images: LDA,  $k$ -NN, and SVMs w/wo spatial information >> demo1.m

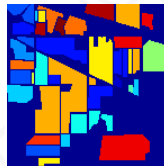
• **Data:**

- Standard image: 16 crop classes, Indiana (USA), 1999.
- AVIRIS sensor: 220 bands,  $145 \times 145$  pixels.

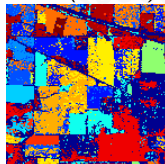
*RGB*



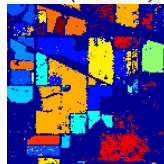
*Ground truth*



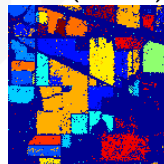
*LDA (59.72%)*



*kNN (86.11%)*



*SVM (88.27%)*



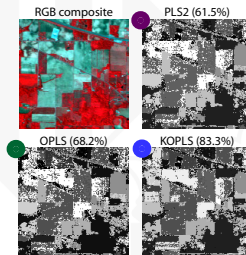
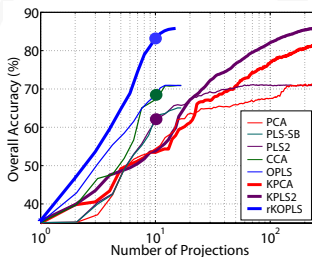
## Practice 2: Feature extraction from hyperspectral images

P2a Extract standard spatial features >> demo2a.m

P2b Extract advanced spectral feature extraction >> demo2a.m

### • Data:

- AVIRIS image taken over NW Indiana's Indian Pine test site in June 1992
- $145 \times 145$  image size, 220 features (bands), 16 land cover classes
- 80% for training and 20% for testing
- Classifier: linear classifier on top of different number of features



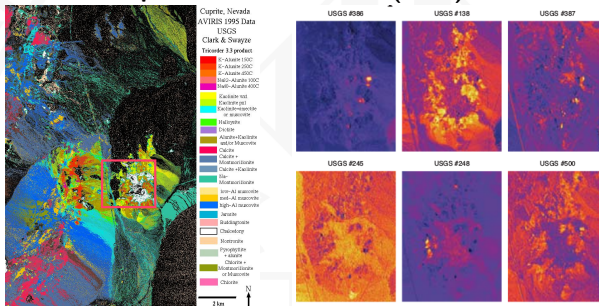
### Practice 3: Evaluate several algorithms for signal unmixing

P3a Signal subspace determination >> demo3a.m

P3b Endmember determination >> demo3b.m

P3c Abundance estimation with unconstrained LS linear regression >> demo3c.m

#### • Data: AVIRIS Cuprite site over Nevada (1995)



**Practice 4:** Evaluate feature extraction and standard supervised classifiers with and without hyperspectral+LiDAR fusion >> demo4.m

- **Data:** Hyperspectral CASI1500 (144 bands in the 380-1050 nm) + LiDAR derived Digital Surface Model (DSM)



## Practice 5: Evaluate the kernel ridge regression to predict Chla, LAI and fCover from hyperspectral images >> demo5.m

- **Data:** SPARC data set (2003, 2004; Barrax, Spain)
  - Field data: Chl measured with CCM-200
  - 30 additional bare soil samples
  - CHRIS mode 1 (62 bands; 34m) nadir spectra

Table 6.1: Correlation coefficient  $R$  results of narrowband and broadband indices proposed in relevant literature tested in the present study along with recent non-parametric models. See [Pereira et al. \[2015\]](#) and references therein.

Method	Formulation	$R$
LR	$R_{\text{RBR}}/R_{\text{RBR}}$	0.52 (0.49)
CV1	$(R_{\text{RBR}} - R_{\text{RBR}})/(R_{\text{RBR}} + R_{\text{RBR}})$	0.66 (0.67)
MaxC	$(R_{\text{RBR}} - R_{\text{RBR}})/(R_{\text{RBR}} + R_{\text{RBR}})$	0.20 (0.29)
MCAR2	$[R_{\text{RBR}} - R_{\text{RBR}}] \cdot [2(R_{\text{RBR}} - R_{\text{RBR}})] / (R_{\text{RBR}} + R_{\text{RBR}})$	0.35 (0.44)
MCAR2	$1.2[2.5(R_{\text{RBR}} - R_{\text{RBR}}) - 1.3(R_{\text{RBR}} - R_{\text{RBR}})]$	0.71 (0.12)
oNDVI	$(R_{\text{RBR}} - R_{\text{RBR}})/(R_{\text{RBR}} + R_{\text{RBR}})$	0.77 (0.12)
oNDVI <sub>max</sub>	$(R_{\text{RBR}} - R_{\text{RBR}})/(R_{\text{RBR}} + R_{\text{RBR}})$	0.80 (0.67)
oNDVI <sub>max</sub>	$(R_{\text{RBR}} - R_{\text{RBR}})/(R_{\text{RBR}} + R_{\text{RBR}})$	0.72 (0.67)
oNDVI	$(R_{\text{RBR}} - R_{\text{RBR}})/(R_{\text{RBR}} + R_{\text{RBR}})$	0.19 (0.20)
oNDVI	$1.2[1.2(R_{\text{RBR}} - R_{\text{RBR}}) - 2.5(R_{\text{RBR}} - R_{\text{RBR}})]$	0.73 (0.67)
NDVI	$(R_{\text{RBR}} - R_{\text{RBR}})/(R_{\text{RBR}} + R_{\text{RBR}})$	0.77 (0.68)
NDVI	$(R_{\text{RBR}} - R_{\text{RBR}})/(R_{\text{RBR}} + R_{\text{RBR}})$	0.81 (0.68)
NPV	$(R_{\text{RBR}} - R_{\text{RBR}})/(R_{\text{RBR}} + R_{\text{RBR}})$	0.72 (0.68)
NPV	$[R_{\text{RBR}} - R_{\text{RBR}}]/[R_{\text{RBR}} + R_{\text{RBR}}]$	0.61 (0.15)
CR-VI	$1.5[1.5(R_{\text{RBR}} - R_{\text{RBR}})/(R_{\text{RBR}} + R_{\text{RBR}}) + 0.35]$	0.79 (0.69)
PR1	$(R_{\text{RBR}} - R_{\text{RBR}})/(R_{\text{RBR}} + R_{\text{RBR}})$	0.77 (0.67)
PR2	$(R_{\text{RBR}} - R_{\text{RBR}})/(R_{\text{RBR}} + R_{\text{RBR}})$	0.76 (0.67)
PSR1	$(R_{\text{RBR}} - R_{\text{RBR}})/R_{\text{RBR}}$	0.79 (0.68)
HDV1	$(R_{\text{RBR}} - R_{\text{RBR}})/\sqrt{(R_{\text{RBR}} + R_{\text{RBR}})}$	0.76 (0.68)
SPV1	$(R_{\text{RBR}} - R_{\text{RBR}})/(R_{\text{RBR}} + R_{\text{RBR}})$	0.79 (0.68)
SPV1	$0.4[2.7(R_{\text{RBR}} - R_{\text{RBR}}) - 1.2(R_{\text{RBR}} - R_{\text{RBR}})]$	0.70 (0.68)
SR	$R_{\text{RBR}}/R_{\text{RBR}}$	0.63 (0.12)
SR1	$R_{\text{RBR}}/R_{\text{RBR}}$	0.74 (0.67)
SR2	$R_{\text{RBR}}/R_{\text{RBR}}$	0.68 (0.69)
SR3	$R_{\text{RBR}}/R_{\text{RBR}}$	0.75 (0.67)
SR4	$R_{\text{RBR}}/R_{\text{RBR}}$	0.76 (0.68)
SRV1	$R_{\text{RBR}}/R_{\text{RBR}}$	0.76 (0.69)
TCAR1	$2(R_{\text{RBR}} - R_{\text{RBR}})[2.2(R_{\text{RBR}} - R_{\text{RBR}}) + R_{\text{RBR}}]$	0.83 (0.13)
TV1	$0.5[12(R_{\text{RBR}} - R_{\text{RBR}}) - 200](R_{\text{RBR}} - R_{\text{RBR}})$	0.70 (0.10)
VOG	$R_{\text{RBR}}/R_{\text{RBR}}$	0.76 (0.68)
VOG2	$(R_{\text{RBR}} - R_{\text{RBR}})/(R_{\text{RBR}} + R_{\text{RBR}})$	0.72 (0.69)
NAOC	Area in RGB TMS	0.76 (0.68)
LR	Least squares	0.88 (0.66)
SVR [Smola and Schölkopf, 2004]	RBF kernel	0.96 (0.63)
SVR [Pereira et al. [2015]]	RBF kernel	0.96 (0.63)
GP [Pereira et al. [2015]]	Anisotropic RBF kernel	0.96 (0.62)

